

Adaptive Filtering for Removing Nonstationary Physiological Noise from Resting State fMRI BOLD Signals

Paolo Piaggi^{1,2*}, Danilo Menicucci^{2,3}, Claudio Gentili⁴, Giacomo Handjaras⁵, Marco Laurino^{2,6}, Andrea Piarulli^{2,3}, Mario Guazzelli⁴, Angelo Gemignani^{2,6}, Alberto Landi^{1,2}

¹Dep. of Energy and Systems Engineering, University of Pisa, Italy.

²EXTREME Centre, Scuola Superiore Sant'Anna, Pisa, Italy.

³Institute of Clinical Physiology, National Research Council (CNR), Pisa, Italy.

⁴Dep. of Psychiatry, Neurobiology, Pharmacology and Biotechnology, University of Pisa, Italy.

⁵Dep. of Experimental Pathology, Medical Biotechnologies, Infectivology and Epidemiology, University of Pisa, Italy.

⁶Dep. of Physiological Sciences, University of Pisa, Italy.

*Email: paolo.piaggi@gmail.com

Abstract—fMRI is used to investigate brain functional connectivity after removing nonneural components by General Linear Model (GLM) approach with a reference ventricle-derived signal as covariate. Ventricle signals are related to low-frequency modulations of cardiac and respiratory rhythms, which are nonstationary activities. Herein, we employed an adaptive filtering approach to improve removing physiological noise from BOLD signals. Comparisons between filtering approaches were performed by evaluating the amount of removed signal variance and the connectivity between homologous contralateral regions of interest (ROIs). The global connectivity between ROIs was estimated with a generalized correlation named RV coefficient. The mean ROI decrease of variance was -52% and -11% , for adaptive filtering and GLM, respectively. Adaptive filtering led to higher connectivity between grey matter ROIs than that obtained with GLM. Thus, adaptive filtering is a feasible method for removing the physiological noise in the low frequency band and to highlight resting state functional networks.

Keywords: *Principal Component Analysis; Adaptive Filtering; Nonstationarity Test; RV coefficient, fMRI BOLD Signal, Resting State, Physiological Noise, Functional Connectivity.*

I. INTRODUCTION

Low frequency fluctuations of Blood Oxygenation Level-Dependent (BOLD) signal in functional Magnetic Resonance Imaging (fMRI) experiments were firstly noticed by Biswal and coworkers as synchronous oscillations between brain regions belonging to the motor network, both within and across hemispheres at rest [1]. This coherence of the spontaneous activities among spatially remote brain areas (i.e. *functional connectivity* [2]) were proved to be mostly limited to frequencies less than 0.1 Hz [3] and it represents the metabolic dynamic of the intrinsic neuronal activity of the brain.

Unfortunately, the BOLD signal contains both neuronal and nonneural components in the low frequency band: main sources of the latter (the so-called *physiological noise*) are related to the low-frequency modulation of cardiac

rhythm [4, 5], respiratory rate [6] and slow variations of arterial carbon dioxide [7]. Very often, instead of considering additional recordings of reference signals of these noise sources (e.g., by means of photoplethysmographs or pneumatic belts), an estimate of these nuisance signals is obtained from BOLD signal itself in nonneural regions such as ventricles (where no neural activity is expected), by means of signals averaging or by using the Principal Component Analysis (PCA).

The contribution of this nonneural confound is typically removed from the functional connectivity estimates by means of linear regression which, in this case, is specifically called “nuisance variable regression” [8]: in practice, the physiological noise signal estimate is included as a regressor in a General Linear Model (GLM) analysis so as to remove its contribution from the selected time course [9].

Aim of this study is to explore the time-frequency characteristics of the physiological noise as estimated from ventricles voxels. Moreover, it was verified whether a more suitable method to remove the physiological noise contribution could be setup. Thus, an adaptive filtering technique - which best deal with nonstationary signals - was employed and compared to the standard GLM approach in order to evaluate their effects on BOLD resting state analyses. Finally, a generalized measure of connectivity between ROIs is also introduced and employed.

II. METHODS

A. Data Acquisition

A 1.5 Tesla GE scanner (General Electric, Milwaukee, WI) was used to acquire basal resting state data (1970 time points) in eight subjects with a GR-EPI sequence (FOV = 24 cm, TR/TE= 300/40 msec, FA = 90°, resolution = 64×64 pixels, voxel size 3,75×3,75×5 mm, REPS = 2000). Four slices aligned to the anterior/posterior commissural line were acquired.

A TR = 300 msec was chosen as sampling time in order to avoid aliasing of cardiac (~1 Hz) and respiratory (0.15-0.40 Hz) components in the low frequency band (<0.1 Hz)

[10]. However, the putative effects of a so short TR was verified by means of several *ad hoc* scan sessions performed with a simple motor task (i.e. finger tapping) at different TR (2000, 500, 300 and 100 msec) and with the same FA, TE and resolution. No significant differences were found in signal change during the tasks across different TR conditions.

For each subjects, a set of high resolution T1 weighted spoiled gradient recall images (1.2 mm thick axial slices; TR = 12.1 ms, TE = 5.22 ms, FA = 20°, FOV = 24 cm, resolution = 256×256 pixels) were also acquired.

Regions of Interest (ROIs) of grey matter were drawn according to available literature suggesting a role in different resting state functional networks [11]. Those included Middle PreFrontal Cortex - MPFC - and insula (default mode network), DorsoLateral PreFrontal Cortex - DLPFC - (dorsal attentional network), Superior Temporal Sulcus - STS - and cuneus (ventral attentional network), white matter (anterior part of the semioval center) and lateral ventricles.

B. Image Preprocessing

Functional data were processed using the Analysis of Functional Neuroimaging (AFNI) software package [12]. This included the compensation of slice-dependent time shift for aligning separate slices to the same temporal origin. Neither spatial smoothing nor motion correction tasks were performed because, for the latter, the maximum displacement of subject head during scan sessions was below 0.7 mm. Data were normalized to stereotaxic coordinates of Talairach and Tournoux atlas [13] and resampled to 1-mm cubic voxels.

C. BOLD Signals Preprocessing

BOLD signals were detrended and filtered for removing cardiac and respiratory physiological components along with ultra-low frequency drifts due to hardware instability. The detrending task consisted in fitting and subtracting polynomials up to eight order while a low-pass Butterworth filter with a cutoff frequency of 0.1 Hz was employed to remove high frequency spurious components. The filter order was set to 10 and a zero-phase digital filtering was obtained by processing the time course in both the forward and reverse directions.

D. Extraction of a Reference Signal for the Physiological Noise

The filtering in the preprocessing allowed the removing of cardiac and respiratory components at their fundamental frequencies. However, other nonneural contributions such as those related to heart beat variability [5] or breath variations [6] were still present in the filtered time courses.

In order to highlight these nuisance components, Principal Component Analysis (PCA) [14] was conducted in order to extract the most representative pattern of the

ventricle time courses. The first principal component of the PCA (which was based on the covariance matrix) was estimated and taken as the reference signal (REF) for the nonneural confound in the slow band.

E. Nonstationarity Test of Reference Signals

For each subjects, REF time course was tested for nonstationary properties using time-frequency surrogates [15, 16]. Namely, for each REF time course, the standard deviation (SD) of signal envelope (derived with the Hilbert transform) was calculated and compared to the SD distribution of 10000 envelope surrogates. Each surrogate of the REF signal was obtained by a phase randomization. Since time-frequency surrogates were proved to be stationary signals [17], the 95th percentile of their SD distribution was used as a threshold to test for REF stationarity, i.e., if REF SD was greater than the 95th percentile of the surrogates distribution, REF time course was considered as nonstationary.

F. Removal of Physiological Noise

Two different methods were employed and compared for removing the physiological noise on the basis of the REF signal:

- a standard GLM approach (the gold standard);
- a novel approach based on the adaptive filtering technique.

For the GLM approach [18] in this fMRI context, a nuisance variable regression analysis [8] was used considering each voxel time course as dependent variable and the REF signal as the only covariate in the model. The estimated values from GLM were then subtracted from the initial time course so as to obtain a filtered version.

On the other hand, REF time course were fed into an adaptive filter as reference signal. The adaptive filter used a Finite Impulse Response (FIR) and transversal structure (tapped delay line) with 20 taps and normalized Least Mean Squared (nLMS) adaptation algorithm [19]. Several runs were conducted to estimate the step size in order to achieve the convergence of the algorithm; in addition, the initial filter coefficients were set to zero values.

G. Functional Connectivity

For each subject, the functional connectivity [2] among brain regions was conducted using all filtered time courses belonging to grey matter (GM) and white matter (WM) regions. Specifically, the correlation between contralateral pairs of ROI (i.e. voxels in right vs. left hemispheres) was assessed to highlight the filtering method which best discriminate among white and grey matter synchronizations, namely, higher (lower) coupling in grey (white) matter, respectively.

To this purpose, the RV coefficient [20] was used to quantify the strength of coupling between ROI pairs as a multivariate generalization of Pearson's correlation coefficient.

Given \mathbf{X} and \mathbf{Y} the signal matrices of right and left hemisphere (\mathbf{X} and \mathbf{Y} have the same time points, i.e. same number of rows, and different number of voxels, i.e. different columns) of a specified ROI whose rows are time points and columns are voxels, RV coefficient (ranging from 0 to 1) is defined as:

$$RV = \frac{\text{trace}(\mathbf{X}\mathbf{X}^T\mathbf{Y}\mathbf{Y}^T)}{\sqrt{[\text{trace}(\mathbf{X}\mathbf{X}^T) \cdot \text{trace}(\mathbf{Y}\mathbf{Y}^T)]}}$$

where *trace* is the sum of diagonal elements of a square matrix.

This multivariate index of correspondence between signal matrices has been already employed in fMRI context to measure the similarity of brain scans between subjects [21] or within subject [22].

H. Statistical Analysis

Repeated measures analysis of variance (ANOVA) was employed to assess differences between filtering methods (GLM and adaptive filtering) and among ROIs.

Objects of the ANOVA were: 1) the variance of the filtered signals; 2) the RV coefficients calculated between contralateral ROIs.

The variance values have been logarithmic transformed so as to correct the skewness of this variable.

Preliminary tests were conducted to check for data normality and homogeneity of variances using Kolmogorov-Smirnov and Levene's tests, respectively.

Post hoc comparisons using the Bonferroni correction of significance were conducted after a significant ANOVA result; eta squared (η^2) index was employed to quantify the effect size in ANOVA model. A *p*-value less than 0.05 was considered statistically significant. Data are presented as mean \pm SEM or mean \pm SD as indicated.

III. RESULTS

A. Extraction of physiological noise estimate

In the eight subjects group, the first principal component (i.e. REF signal) of ventricle time courses explained $46.0\% \pm 18.7\%$ (mean \pm SD) of the global signals variance in that region. Figure 1 shows the first 10 eigenvalues of single subject PCA with their 95% confidence interval: no error bar belonging to the first eigenvalue overlap with those related to the second element ($p < 0.05$). These results indicate that the first principle component can be considered a good estimation of the physiological noise of ventricle signals.

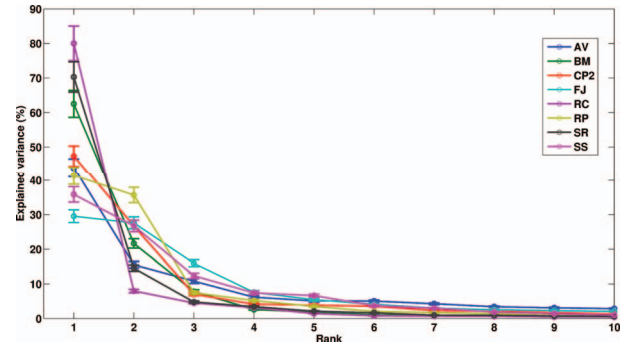


Figure 1. Scree plot of single subject PCA. Error bars of each eigenvalue were drawn from its 95% confidence interval [14].

B. Time-frequency analysis of REF signals

For each subject, the SD of REF envelope was computed and compared to those obtained from 10000 time-frequency surrogates: in all subjects, the SD of REF time course was greater than the 95th percentile of distribution of its surrogates, proving that REF signal is a nonstationary signal (Table 1).

TABLE I. PCA AND NONSTATIONARITY TEST RESULTS OF REF TIME COURSE

Subject	N° of Ventricle Voxels	Exp. Variance of 1° PC (%)	SD of 1° PC Envelope	95° Percentile of Surrogates SD Distribution
AV	87	31.0	11.72	9.96
BM	76	60.0	64.39	45.06
CP2	107	39.8	22.94	18.66
FJ	74	23.9	15.83	12.05
RC	133	76.2	72.76	55.11
RP	122	39.1	53.46	44.99
SR	73	65.3	31.63	29.29
SS	62	32.8	28.29	17.23

C. Filtering based on REF time course

REF time course was employed as either the only covariate in the GLM analysis or as the reference signal in the adaptive filtering algorithm. For each voxel time course, the difference between signal variances before and after the filtering stage was computed and normalized to pre-filtering value ($\Delta\text{var}\%$).

Figure 2 shows $\Delta\text{var}\%$ for the selected ROIs after removing REF contribution from each time course with both methods. As expected, the greatest reduction was noticed for ventricle voxels which were filtered with their 1° PC (i.e. the REF signal). Adaptive filtering (blue line) shows a larger reduction of signals variance with respect to GLM analysis (green line). The comparison between filter methods performed with the ANOVA yielded a significant global decreases of -52% and -11% , respectively with $p < 0.001$ and $\eta^2 = 63\%$.

Figure 3 shows post-filtering residual variance after GLM and adaptive filtering approaches. In both approaches,

white matter variance was lower than that of grey matter regions (Bonferroni adjusted $p < 0.05$): in particular, variance of cuneus voxels were the most greater among neural ROIs (adj. $p < 0.05$). Furthermore, for each method the variance of BOLD signals belonging to ventricles was still greater than those observed in white and grey matter regions (adj. $p < 0.001$) according greater initial variance of these signals (Table 1).

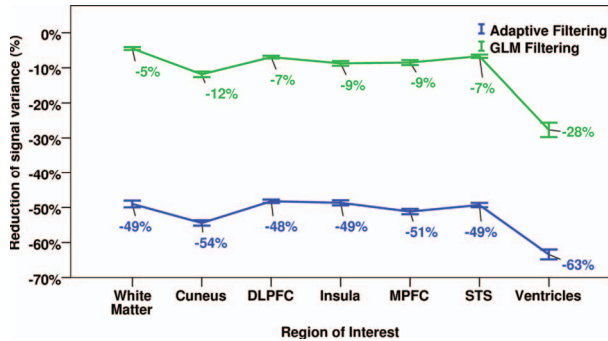


Figure 2. Reductions of BOLD signal variance using REF time course.

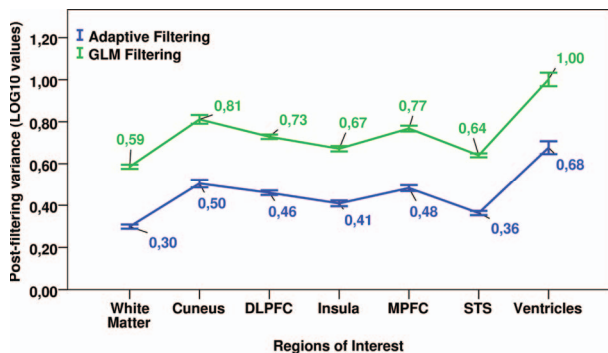


Figure 3. Post-filtering BOLD signal variance for each selected ROIs.

D. Functional connectivity

The functional connectivity of contralateral ROIs in the eight subjects was quantified by the RV coefficient. It was calculated in three conditions: using the pre-filtered only time courses (orange line); after GLM filtering (green lines) and after adaptive filtering (blue line) (Figure 4).

On average, adaptive filtering showed mean RV coefficients greater than the other conditions. (adj. $p < 0.05$). In addition after adaptive filtering of REF signal, ventricles spurious coupling was lower than the other measures while GM functional connectivity was higher than within WM (with the exception of cuneus and STS). Furthermore, adaptive filtering provides a better contrast among ROIs ($\eta^2 = 29\%$) than GLM filtered ($\eta^2 = 25\%$) and pre-filtered only signals ($\eta^2 = 12\%$).

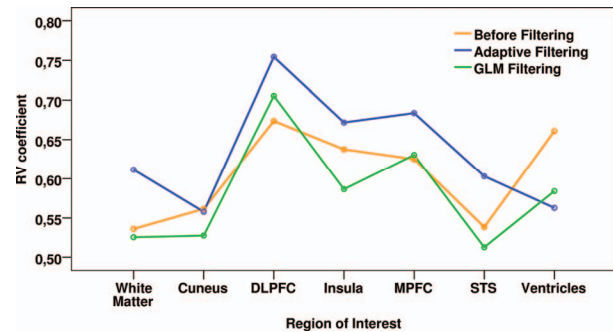


Figure 4. Mean RV coefficients of contralateral ROIs in eight subjects.

IV. CONCLUSIONS

Time courses obtained from PCA of ventricles in the low frequency band were proved to be nonstationary signals. For this reason, an adaptive filtering approach could take into account this time-frequency properties and better removed the physiological noise from other voxels in the brain at rest. Indeed, the adaptive filtering technique removed a greater amount of signal variance in each ROIs than the standard GLM filtering (-52% and -11% , respectively); in addition, the functional connectivity estimated by using RV coefficient on contralateral ROIs showed that adaptive filtering led to higher coupling in grey matter ROIs than those obtained with GLM analysis.

These results suggest that adaptive filtering may be a feasible approach for removing the physiological noise in the low frequency band and to highlight resting state functional networks.

REFERENCES

- [1] B. Biswal, *et al.*, "Functional connectivity in the motor cortex of resting human brain using echo-planar MRI," *Magn Reson Med*, vol. 34, pp. 537-41, Oct 1995.
- [2] K. J. Friston, "Functional and effective connectivity in neuroimaging: A synthesis," *Human Brain Mapping*, vol. 2, pp. 56-78, 1994.
- [3] D. Cordes, *et al.*, "Mapping functionally related regions of brain with functional connectivity MR imaging," *AJNR Am J Neuroradiol*, vol. 21, pp. 1636-44, Oct 2000.
- [4] C. Chang, *et al.*, "Influence of heart rate on the BOLD signal: the cardiac response function," *Neuroimage*, vol. 44, pp. 857-69, Feb 1 2009.
- [5] K. Shmueli, *et al.*, "Low-frequency fluctuations in the cardiac rate as a source of variance in the resting-state fMRI BOLD signal," *Neuroimage*, vol. 38, pp. 306-20, Nov 1 2007.
- [6] R. M. Birn, *et al.*, "Separating respiratory-variation-related fluctuations from neuronal-activity-related fluctuations in fMRI," *Neuroimage*, vol. 31, pp. 1536-48, Jul 15 2006.
- [7] R. G. Wise, *et al.*, "Resting fluctuations in arterial carbon dioxide induce significant low frequency variations in BOLD signal," *Neuroimage*, vol. 21, pp. 1652-64, Apr 2004.
- [8] T. E. Lund, *et al.*, "Non-white noise in fMRI: does modelling have an impact?," *Neuroimage*, vol. 29, pp. 54-66, Jan 1 2006.
- [9] M. D. Fox, *et al.*, "The human brain is intrinsically organized into dynamic, anticorrelated functional networks," *Proc Natl Acad Sci U S A*, vol. 102, pp. 9673-8, Jul 5 2005.

- [10] T. E. Lund, "fcMRI--mapping functional connectivity or correlating cardiac-induced noise?," *Magn Reson Med*, vol. 46, pp. 628-9, Sep 2001.
- [11] M. D. Fox and M. E. Raichle, "Spontaneous fluctuations in brain activity observed with functional magnetic resonance imaging," *Nat Rev Neurosci*, vol. 8, pp. 700-11, Sep 2007.
- [12] R. W. Cox, "AFNI: software for analysis and visualization of functional magnetic resonance neuroimages," *Comput Biomed Res*, vol. 29, pp. 162-73, Jun 1996.
- [13] J. Talairach and P. Tournoux, *Co-planar stereotaxic atlas of the human brain: 3-dimensional proportional system : an approach to cerebral imaging*: G. Thieme, 1988.
- [14] I. T. Jolliffe, *Principal component analysis*: Springer-Verlag, 2002.
- [15] P. Borgnat, *et al.*, "Testing Stationarity With Surrogates: A Time-Frequency Approach," *Signal Processing, IEEE Transactions on*, vol. 58, pp. 3459-3470, 2010.
- [16] T. Schreiber and A. Schmitz, "Surrogate time series," *Physica D: Nonlinear Phenomena*, vol. 142, pp. 346-382, 2000.
- [17] C. Richard, *et al.*, "Statistical hypothesis testing with time-frequency surrogates to check signal stationarity," in *Acoustics Speech and Signal Processing (ICASSP), 2010 IEEE International Conference on*, 2010, pp. 3666-3669.
- [18] K. J. Friston, *et al.*, "Analysis of fMRI time-series revisited," *Neuroimage*, vol. 2, pp. 45-53, Mar 1995.
- [19] S. S. Haykin, *Adaptive filter theory*: Prentice Hall, 2002.
- [20] P. Robert and Y. Escoufier, "A Unifying Tool for Linear Multivariate Statistical Methods: The RV- Coefficient," *Journal of the Royal Statistical Society. Series C (Applied Statistics)*, vol. 25, pp. 257-265, 1976.
- [21] F. Kherif, *et al.*, "Group analysis in functional neuroimaging: selecting subjects using similarity measures," *Neuroimage*, vol. 20, pp. 2197-208, Dec 2003.
- [22] H. Abdi, *et al.*, "How to compute reliability estimates and display confidence and tolerance intervals for pattern classifiers using the Bootstrap and 3-way multidimensional scaling (DISTATIS)," *Neuroimage*, vol. 45, pp. 89-95, Mar 1 2009.